Bypassing Transients of Pre-Insertion Resistor during Energization of MMC-HVDC Stations

Lina He, *Member, IEEE*

***Abstract*—In a modular multilevel converter (MMC) station, a circuit breaker (CB) with a pre-insertion resistor (PIR) is required to be installed to suppress the inrush current due to the saturation of the converter transformer during the energization of the MMC station. The insertion time of the PIR depends on the specific design of the MMC-HVDC projects, usually in the order of seconds. When the PIR is bypassed from the energization circuit, the resulting switching transients can lead the converter transformer to be saturated. The caused high inrush currents are able to endanger the MMC station and reduce the transformer life-cycle. In order to understand the corresponding transients and perform the simulation study, this paper presents a test model, including a MMC station, a HVDC feeder and an external network. Two cases with different bypassing strategies are simulated in this paper to identify an appropriate bypassing time.**

***Index Terms*—Pre-insertion resistor, energization of MMC station, transformer saturation, Inrush current.**

I. Introduction

The MMC-HVDC technology has been applied for network interconnection and offshore wind power integration due to its typical advantages, including fast and independent control of active and reactive power, feasibility of multi-terminal dc grids, and black start capability [1-3]. The MMC-HVDC link called BorWin2 in North Sea can be an example. It connects the Global Tech 1 offshore wind farm to mainland Germany via a dc cable connection with a length of 200 km [4].

In a MMC-HVDC station, the power converter is connected to a HVDC feeder via a transformer. When a CB on the HVDC feeder is switched on to energize the MMC station, the caused abrupt voltage change can lead to the saturation of the converter transformer. Thus, high inrush currents appear. The magnitudes of those inrush currents can be up to several times of the rated current of the converter transformer in severe situations. They can damage the devices of power grids or even endanger power system security.

In order to counteract those accompanied dangerous transients during energization, the CB with a PIR is required to be installed in the MMC-HVDC station. In the present MMC-HVDC projects, e.g., HVDC PLUS from Siemens, the CB with a PIR is located between the power converter and the transformer. Before the converter station is energized, the PIR needs to be connected to the circuit with the paralleled CB switched off. It is aimed to suppress the possible transformer inrush currents generated during energization. The corresponding transient performance has been analyzed in [5].

In the existing MMC-HVDC projects, the resistance of the PIR can be up to thousands of Ohms. It depends on the circuit design of the specific MMC-HVDC projects. When the PIR with a large resistance is bypassed from the circuit, a dc component flux has to be generated simultaneously to maintain the flux continuity. The dc component flux has the identical magnitude of the difference of the fluxes before and after the PIR bypassing, but with the opposite direction. Its amplitude can be affected by the bypassing time of the PIR. This dc component can lead to the second saturation of this converter transformer and reduce the life-cycle of the transformer. The resulting transients are analyzed in this paper.

In the existing literatures, only a couple studies have investigated the energization of the HVDC station. The study of [6] analyzed the energization performance of the three-level voltage source converter (VSC)-HVDC connection. The reference of [5] discussed the impact of the PIR on the mitigation of transformer inrush currents. However, the transient behavior of the bypassing of the PIR during the energization of the MMC station has not been studied yet, to the best of the author's knowledge. The resulting impact of the dc component caused during the energization of the MMC-HVDC station can be significant. It needs to be addressed to ensure security of power system devices. To fill this gap, this paper analyzes the caused transient behavior by the PIR bypassing and identifies an appropriate bypassing time.

The structure of this paper is as follows. The system model for the energization simulation of the MMC station is developed in Section II, including a MMC station, a HVDC feeder and an external network. The simulation cases are performed in Section III to analyze the resulting transient behavior by bypassing the PIR during the energization of the MMC station. In addition, an appropriate bypassing time of the PIR is also determined in Section III. Section IV concludes.

II. System Model during Energization

A simulation system is modeled in this section to analyze the transient behavior caused by the bypassing of the PIR during the energization of the MMC station. Its configuration is shown in Fig. 1. In this model, the network is represented by a Thevenin equivalent circuit. The HVDC feeder consists of a CB

Lina He is with Department of Electrical and Computer Engineering, University of Illinois at Chicago, Chicago, (e-mail: lhe@uic.edu).

and a cable/overhead line (OHL). The cable/OHL is modeled as a series-connected Pi circuit. Each Pi circuit corresponds to a segment of the transmission line with a short length. The MMC station contains a transformer, a CB with a PIR and a MMC converter.

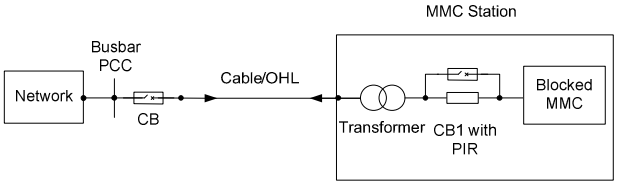

Fig. 1 System model of MMC station for energization

A. MMC Modeling

During the energization of a MMC station, the power converter needs to be blocked by switching off all the power semiconductors in six converter arms. The applied power semiconductors are usually the insulated gate bipolar transistor (IGBT) with turn-off capability. With all the semiconductors switched off, the MMC converter becomes an uncontrollable diode bridge. Its switching operation depends on the instantaneous voltage difference between two terminals. Thus, the blocked power converter cannot be controlled any more, losing the control capability.

Differing from the two or three-level VSC based HVDC, the MMC-HVDC station is not equipped with an ac filter. Therefore, the generated lower-order harmonics cannot be eliminated, resulting in waveform distortions. The caused waveform distortions can impact the power quality of the connected ac network. In addition, these lower-order harmonics could intensify the saturation of the converter transformer, leading to more severe inrush currents. As a result, the PIR is required to be connected during the energization of a MMC-HVDC station to eliminate the inrush currents and avoid device damage.

The configuration of a half-bridge MMC is shown in Fig. 2 (a). It is a three-phase bridge that consists of six converter arms. Each arm is formed by a number of identical but individually controllable submodules (SMs) and a reactor. The submodule contains an IGBT half bridge as a switching element and a capacitor unit for energy storage. The detailed circuit configuration is illustrated in Fig. 2 (b) [7].

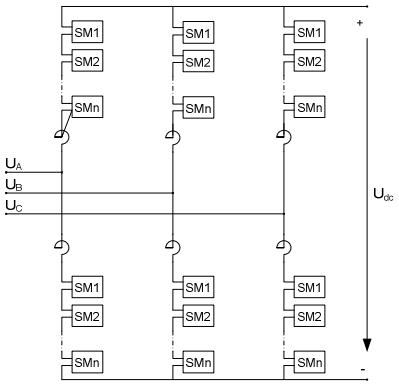

(a)

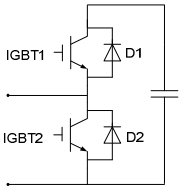

(b)

Fig. 2 (a) MMC configuration, and (b) submodule of MMC

This submodule can be operated in three different states, including capacitor-on, capacitor-off and energization. In the state of capacitor-on, the voltage of storage capacitor in Fig. 1 (b) is applied to the terminals of the submodule. Depending on the flow direction, the current circulates either through D1 to charge the capacitor, or through IGBT1 to discharge the capacitor. For the status of capacitor-off, the current flows through IGBT2 or D2 that makes the voltage crossing the submodule terminals be zero. In this situation, the capacitor voltage remains unchanged. During the operation of MMC-HVDC, each submodule in a converter arm is individually selected and controlled. With the appropriate control strategy, the MMC can provide a fine gradation of the output voltage. The more steps are used, the proportion of harmonics is smaller and the high-frequency noise is lower. Thus, each converter arm can be represented as a controllable voltage source if it consists of enough submodules. By adjusting the ratio of the converter arm voltages in each phase, the desired sinusoidal voltage at the ac terminal is able to be achieved. Therefore, it is not necessary to equip an ac filter with the MMC converter.

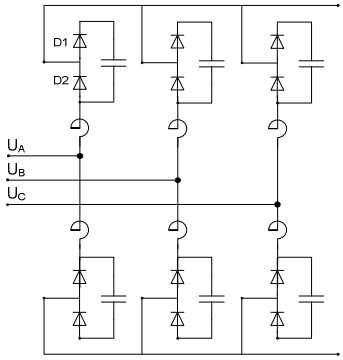

Fig. 3 Electromagnetic transient model of MMC during energization

During the energization of a MMC station, both IGBTs in each submodule are switched off. When the CB on the HVDC feeder is switched on for energization, the current flows from the ac terminal to the positive dc pole to charge the capacitor. If the current flows in the opposite direction, the freewheeling diode D2 bypasses the capacitor. As a result, the converter circuit during the status of energization becomes a diode bridge. The voltages of converter arms cannot be controlled any more. By aggregating all the submodules in each converter arm, the electromagnetic transient model of the MMC converter can be represented in Fig. 3. It is seen that the MMC converter behaves as a three-phase uncontrollable diode bridge during its energization.

B. CB with PIR

The configuration of the CB with a PIR is illustrated in Fig. 4. It is shown that the PIR and switch s1 are in parallel with the CB1. Before energization, the PIR needs to be connected by closing switch s1. After a selected insertion time, the CB1 is switched on to bypass the PIR to improve the energization efficiency. The status of the switch s1 is not changed after the CB1 is switched on, i.e., the PIR remains connected during operation.

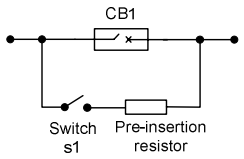

Fig. 4 Model of CB with a PIR

C. Transformer Modeling

The energization transients range in the level of low/medium frequency. Therefore, the transformer during energization can be modeled as a lumped parameter model [8]. Its single phase model is shown in Fig. 5. In this model, the R-L circuit is applied to ensure the appropriate frequency response of the transformer, and the magnetizing branch is utilized to perform the saturation characteristic of the transformer.

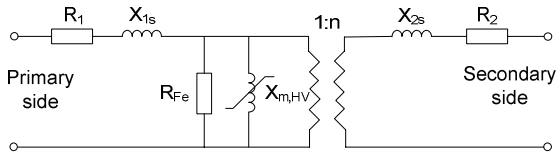

Fig. 5 Single phase model of transformer

In the primary side, the symbols R_1 and X_{1s} correspond to the resistance and leakage reactance of the primary winding, respectively. The magnetizing branch is represented by the transformer core resistance R_{Fe} and magnetizing reactance X_m. In the secondary side, the symbols R_2 and X_{2s} indicate the resistance and leakage reactance of the secondary winding, respectively. In the transformer model, the saturation characteristic can be modeled as a simplified two-slope piecewise linear function, as shown in Fig. 6.

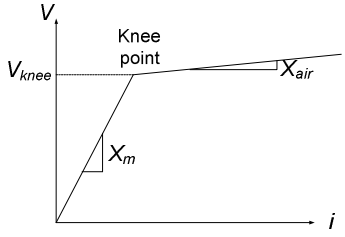

Fig. 6 Simplified two-slope magnetizing characteristic

It is seen in Fig. 6 that the slope of the line is equal to the magnetizing reactance X_m when the transformer voltage is under the saturation knee point V_{knee}. After the transformer is saturated, the magnetizing reactance is dramatically reduced to the air-core reactance X_{air}, thus resulting in an inrush current in this branch. The magnitude of the inrush current can be up to several times of the rated transformer current. It causes the crossing voltage of the primary side of the transformer to be large and leads to the voltage dip at the point of common coupling (PCC) of the HVDC feeder.

III. Case Studies

A. Simulation Data

The system model is developed on the Siemens PTI software PSS®NETOMAC (Version 12.5) for time-domain simulation. The applied parameters are listed in Appendix, including the network, the converter transformer, the MMC converter and the PIR. The cable is with the length of 0.671 km. Its resistance, reactance and capacitance per km are 0.037 Ohm, 0.11 Ohm and 230 nF, respectively. The applied remanence flux of the transformer in phase A is -0.8 p.u. to perform the worst saturation case, and the corresponding remanence fluxes in phases B and C are 0.4 p.u..

The relationship between the voltage of the magnetizing branch of the transformer and the flux of the transformer core is represented below,

$$V = d\psi/dt \quad (1)$$

It is found that the phase angle of the flux (ψ) is behind the phase angle of the voltage (V) by 90 degrees. When the PIR is bypassed at a zero-crossing of the voltage of the PCC point, the corresponding flux in the transformer core has the maximum magnitude. In order to maintain the continuity of the flux at the bypassing instant, a dc component flux has to be generated simultaneously. Its magnitude is equal to the difference of the fluxes before and after the PIR bypassing. Thus, with consideration of the magnitude of the flux after the PIR bypassing to be a constant, the generated dc component flux has the maximum magnitude when the PIR is bypassed at the zero-crossing of the PCC voltage.

In the simulation, the CB is switched on at a zero-crossing of the phase A-to-ground voltage of the PCC, i.e., 0.1 s, to energize the MMC station. After the voltages of the dc poles rise to 1 p.u., the CB1 is switched on to bypass the PIR. In order to analyze the transient behavior caused by the bypassing of the PIR, and meanwhile determine an appropriate bypassing time, the PIR bypassing cases are performed at both the zero-crossing and maximum of the PCC voltage. According to the analysis in the last paragraph, the dc components caused in these two cases will be with the maximum and minimum magnitudes, respectively. For the other cases with the different bypassing time, the amplitudes of the caused dc components are between the maximum and minimum magnitudes in these two cases. Therefore, it is not necessary to involve other simulation cases in this section.

B. Bypassing at the Zero-crossing of PCC Voltage in Phase A

In this simulation case, the PIR is bypassed at a zero-crossing of the phase A-to-ground voltage of the PCC. The simulation results are reported in Fig. 7, including the transformer flux, the inrush currents flowing through the

magnetizing branch of the transformer, the dc pole voltages of the converter, the PCC voltages and the enlarged PCC voltages around the bypassing time. It is seen in Fig. 7 (a) that the transformer is slightly saturated after the CB is switched on. The orange horizontal lines shown in this figure indicate the saturation limit of the converter transformer, which is 1.195 p.u.. With the time goes, the voltages of the dc poles shown in Fig. 7 (c) rise slowly and reach 1 p.u. at about 1.8 s.

It is shown in Fig. 7 (e) that the CB1 is switched on to bypass the PIR at a zero-crossing of the phase A-to-ground voltage of the PCC, i.e., 2.005 s. This switching behavior causes the transformer to be saturated again, as seen in Fig. 7 (a) and (b). It is seen in Fig. 7 (b) that the caused inrush current in phase A by the bypassing of the PIR is up to 0.24 kA, which is much higher than that caused by the CB switching. It is also found in Fig. 7 (b) that the inrush current in phase A contains a dc component with a slow decay rate. In case of an unexpected failure on the HVDC feeder, the dc component can lead to current zero-crossing missing phenomena, thus resulting in a CB breaking failure. The related study about the current zero-crossing missing can be found in [9].

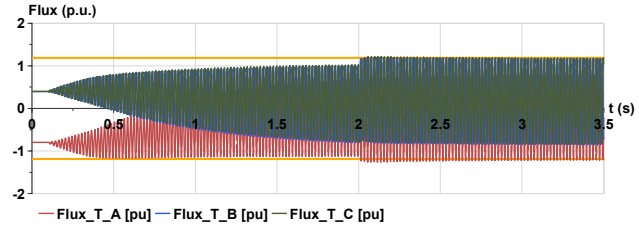

(a)

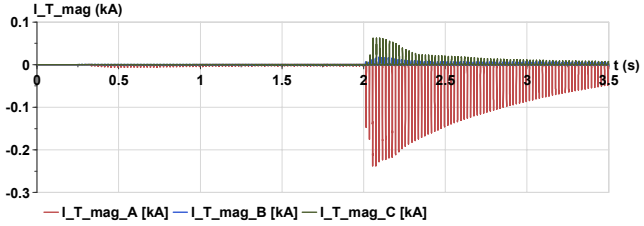

(b)

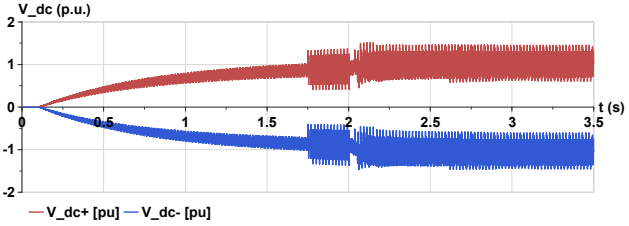

(c)

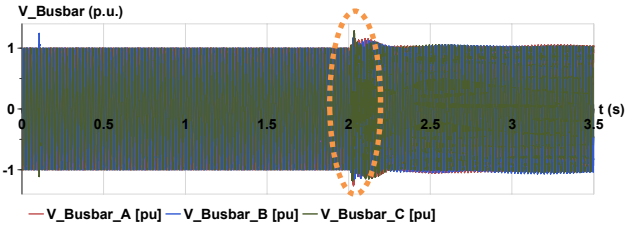

(d)

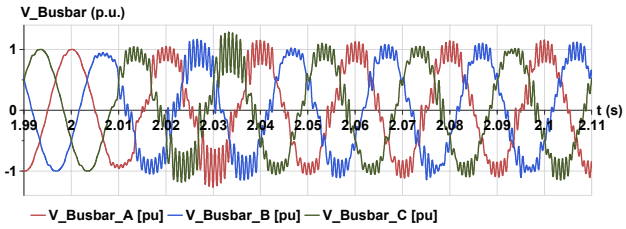

(e)

Fig. 7 Simulation results of case B: (a) flux of converter transformer; (b) inrush currents flowing through magnetizing branch of transformer; (c) dc pole voltages of converter; (d) busbar voltage; (e)enlarged PCC voltage around bypassing time.

C. Bypassing at the Maximum of PCC Voltage in Phase A

The PIR in this case is bypassed at the maximum of the phase A-to-ground voltage of the PCC. The simulation results are illustrated in Fig. 8. Same as Fig. 7, Fig. 8 includes the transformer flux, the inrush currents flowing through the magnetizing branch of the transformer, the dc pole voltages of the converter, the PCC voltages and the enlarged PCC voltages around the bypassing time.

Differing from the case in Section III B, the CB1 is switched on to bypass the PIR at the maximum value of the phase A-to-ground voltage of the PCC, i.e., 2 s, as shown in Fig. 8 (e). It can be seen in Fig. 8 (a) that the transformer is saturated slightly when the PIR is bypassed by switching on CB1. The resulting inrush current in phase A has a peak value of 0.022 kA as shown in Fig. 8 (b), which is much lower than that in the simulation case of section III B. Therefore, in order to avoid the unexpected high inrush current, the PIR needs to be bypassed at the maximum of the PCC voltage.

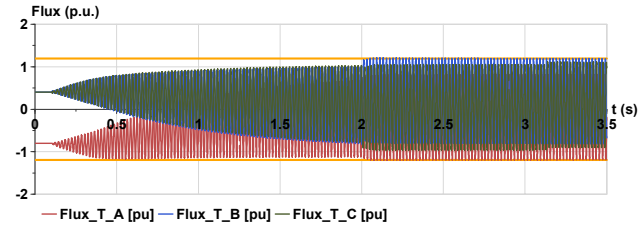

(a)

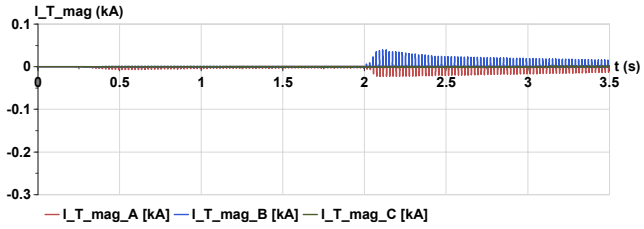

(b)

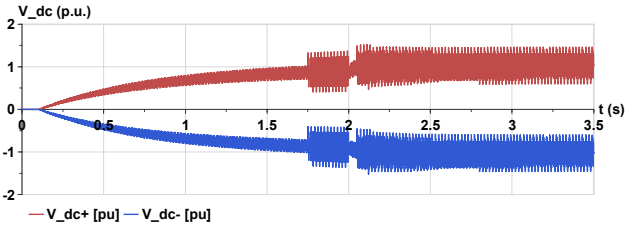

(c)

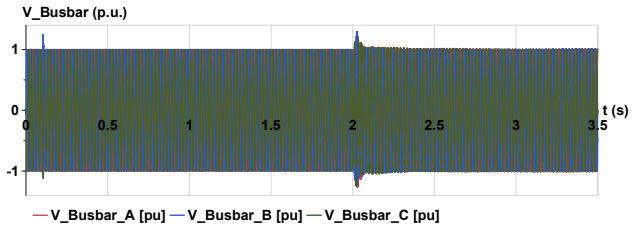

(d)

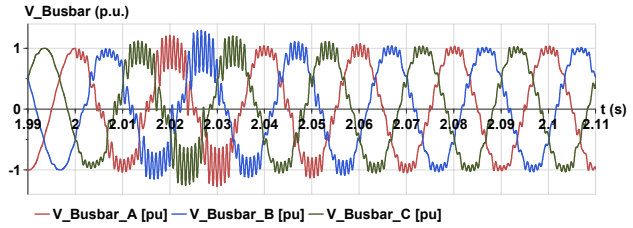

(e)

Fig. 8 Simulation results of case C: (a) flux of converter transformer; (b) inrush currents flowing through magnetizing branch of transformer; (c) dc pole voltages of converter; (d) busbar voltage; (e) enlarged PCC voltages around bypassing time.

IV. Summary of Results

The CB with a PIR is installed in the MMC station to eliminate the inrush current caused by the saturation of the converter transformer during energization. After a selected insertion time, the PIR is bypassed from the energization circuit. The bypassing time of the PIR can impact the transient behavior significantly. This paper has performed two cases with the bypassing time at the zero-crossing and the maximum of the PCC voltage, respectively. The generated dc components in these two cases correspond to the maximum and minimum magnitudes, respectively. The phase A is chosen in the simulation as an example. It is found that both of the bypassing cases can cause the saturation of the converter transformer. However, the case with the bypassing time at the zero-crossing of the PCC voltage leads to a much higher inrush current than the case with the bypassing time at the maximum of the PCC voltage. Therefore, it is recommended during the energization of the MMC station to bypass the PIR at the maximum of the PCC voltage to avoid the transformer saturation and possible damage.

V. Appendix

TABLE I
PARAMETERS OF NETWORK

Descriptions	Values	Units
Rated voltage	400	kV
Rated frequency	50	Hz
Three-phase initial symmetrical short-circuit current	2.89	kA
X/R ratio	0.1	-

TABLE II
PARAMETERS OF TRANSFORMER

Descriptions	Values	Units
Rated apparent power	630	MVA
Rated voltage of high voltage (HV) winding	400	kV
Rated voltage of low voltage (LV) winding	332	kV
Short-circuit impedance	19.48	%
Resistive part of short-circuit impedance	1.137	%
Iron losses	205	kW
No-load current	0.102	%
u_k division between HV and LV windings	0.5	-
Air-core reactance	111	Ohm
Saturated flux magnitude density	1.96	T
Rated flux magnitude density	1.64	T
Vector group	YNyn0	-

TABLE III
PARAMETERS OF MMC CONVERTER

Descriptions	Values	Units
Inductance of each converter arm	53.9	mH
Aggregated capacitance of each converter arm	50	μF
Pre-insertion resistor of CB	1980	Ohm

References

[1] L. He and C.-C. Liu, "Parameter identification with PMUs for instability detection in power systems with HVDC integrated offshore wind energy," *IEEE Transactions on Power Systems*, vol. 29, no.2, Mar. 2014.

[2] L. He, C.-C. Liu, A. Pitto, and D. Cirio, "Distance protection of AC grid with HVDC- connected offshore wind generators," *IEEE Transactions on Power Delivery*, vol. 29, no.2, Apr. 2014.

[3] K. Bell, D. Cirio, A.M. Denis, L. He, C.-C. Liu, C. Moreira, and P. Panciatici, "Economic and technical criteria for designing future offshore HVDC grids," *IEEE PES*: Innovative Smart Grid Technologies, Gothenburg, Sweden, 2010.

[4] WindEnergy Network – Communication hub for the wind energy industry, *www.windenergynetwork.co.uk*, Mar. 2015.

[5] L.He, "Effects of pre-insertion resistor on energization of MMC-HVDC stations," *2017 IEEE PES General Meeting*, Chicago, IL, Jul. 2017.

[6] N. Singh, and J. Carlsson, "Energization study of five-terminal multi-level HVDC converter station," *2013 IEEE PES General Meeting*, Vancouver, BC, Canada, Jul. 2013.

[7] J. Peralta, H. Saad, S. Dennetiere, J. Mahseredjian, and S. Nguefeu, "Detailed and averaged models for a 401-level MMC-HVDC system", *IEEE Transactions on Power Delivery*, vol. 27, no.3, Jul. 2012.

[8] J. Martinez, and B. Mork, "Transformer modeling for low- and mid-Frequency transients – a review," *IEEE Transactions on Power Delivery*, vol. 20, no.2, Apr. 2005.

[9] L. He and R. Voelzke, "Effects of pre-insertion resistor on energization of compensated Lines," *2016 IEEE PES General Meeting*, Boston, MA, Jul. 2016.

Lina He (SM'11-M'13) received her Ph.D. degree in electrical engineering at University College Dublin, Ireland in 2014. She is currently an Assistant Professor in the department of Electrical and Computer Engineering at University of Illinois of Chicago, Chicago, IL. She was a Senior Consultant at Siemens headquarter in Germany and Siemens US from 2014 to 2017. She was also an Electrical Engineer at Tractebel Engineering, Brussels in 2014 and at State Grid Corporation of China, China during 2009-2010. Her research interests include renewable energy integration, power electronics and its applications in power systems, smart grid, wide-area protection and control, phasor measurement unit, HVDC control and operation, power system modeling and analysis, power system resilience, and power system electromagnetic transient modeling and analysis.